



THE UNIVERSITY *of* EDINBURGH

Edinburgh Research Explorer

Anion-ordered chains in a d1 perovskite oxynitride: NdVO₂N

Citation for published version:

Oró-solé, J, Clark, L, Bonin, W, Attfield, JP & Fuytes, A 2013, 'Anion-ordered chains in a d1 perovskite oxynitride: NdVO₂N' Chemical Communications, vol. 49, no. 24, pp. 2430. DOI: 10.1039/c3cc38736d

Digital Object Identifier (DOI):

[10.1039/c3cc38736d](https://doi.org/10.1039/c3cc38736d)

Link:

[Link to publication record in Edinburgh Research Explorer](#)

Document Version:

Peer reviewed version

Published In:

Chemical Communications

Publisher Rights Statement:

Copyright © 2013 by the Royal Society of Chemistry. All rights reserved.

General rights

Copyright for the publications made accessible via the Edinburgh Research Explorer is retained by the author(s) and / or other copyright owners and it is a condition of accessing these publications that users recognise and abide by the legal requirements associated with these rights.

Take down policy

The University of Edinburgh has made every reasonable effort to ensure that Edinburgh Research Explorer content complies with UK legislation. If you believe that the public display of this file breaches copyright please contact openaccess@ed.ac.uk providing details, and we will remove access to the work immediately and investigate your claim.



Post-print of a peer-reviewed article published by the Royal Society of Chemistry.

Published article available at: <http://dx.doi.org/10.1039/C3CC38736D>

Cite as:

Oró-solé, J., Clark, L., Bonin, W., Attfield, J. P., & Fuertes, A. (2013). Anion-ordered chains in a d1 perovskite oxynitride: NdVO₂N. *Chemical Communications*, 49(24), 2430.

Manuscript received: 05/12/2012; Accepted: 05/02/2013; Article published: 06/02/2013

Anion-ordered chains in a d¹ perovskite oxynitride: NdVO₂N**

Judith Oró-Solé,¹ Lucy Clark,² William Bonin¹ J. Paul Attfield^{2,*} and Amparo Fuertes^{1,*}

^[1]Institut de Ciència de Materials de Barcelona (ICMAB-CSIC), Campus UAB, 08193 Bellaterra, Spain.

^[2]EaStCHEM, School of Chemistry and CSEC, Joseph Black Building, University of Edinburgh, West Mains Road, Edinburgh, EH9 3JJ, UK.

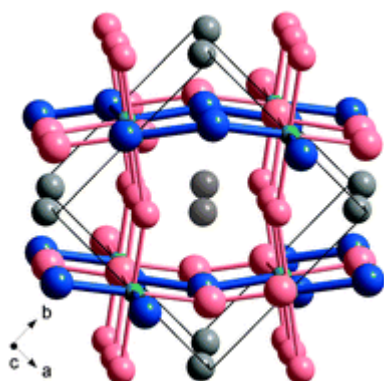
^[*]Corresponding authors; A.F. e-mail: amparo.fuertes@icmab.es, fax: +34 935805729, tel: +34 935801853; J.P.A. e-mail: j.p.attfield@ed.ac.uk, fax: +44 (0)1316517049, tel: +44 (0)1316517229

^[**]We thank Dr Kevin Knight for assistance with neutron data collection at ISIS. This work was supported by the Spanish Ministerio de Economía y Competitividad, Spain (Projects MAT2011-24757 and SAB2011-0047) and EPSRC, the Leverhulme Trust and the Royal Society, UK.

Supporting information:

^[†] Electronic supplementary information (ESI) available: Details of the synthesis, analysis, structural characterisations, and property measurements. See <http://dx.doi.org/10.1039/C3CC38736D>

Graphical abstract:



Abstract

The correlated anion order in the oxynitride perovskite NdVO_2N , where disordered zig-zag VN chains segregate into planes within a pseudo-cubic lattice, is similar to that in materials such as SrTaO_2N containing d^0 transition metal cations. However, NdVO_2N has $3d^1 \text{V}^{4+}$ cations and the 3d-electrons are itinerant, showing that the anion chain order in oxynitride perovskites is robust to electron-doping.

Main text

The d^n electron configurations of transition metal cations have a profound influence on the properties of their solid compounds. d^0 phases are typically wide-bandgap insulators, and off-centre (locally acentric) cation displacements resulting from second order Jahn–Teller (SOJT) effects can give rise to ferroelectricity. In contrast, materials with $n > 0$ electrons often show magnetic and conducting phenomena, and centric first order Jahn–Teller (FOJT) distortions for degenerate d^n configurations. An unusual correlated anion order driven by d^0 effects was recently discovered in oxynitride perovskites of high valent transition metals.¹ These AMo_2N or AMON_2 materials are insulators with notable optical, photocatalytic, and dielectric properties.^{2,3} Although a full long-range anion order is not observed in these materials, the recent neutron and electron diffraction analysis of SrMO_2N ($M = \text{Nb}, \text{Ta}$)¹ showed that well-defined *cis*- MO_4N_2 octahedra are present, resulting in disordered zig-zag MN chains that segregate into two-dimensional perovskite layers. Covalent SOJT type d^0 effects favour the local *cis*- MN_2O_4 configurations, as nitride is more strongly bonded to the M cations than oxide. Unusual sub-extensive configurational entropies that vary with particle size and tend to zero per atom in macroscopic samples are predicted for these correlated anion orders.⁴

Non-stoichiometry can introduce electron carriers into oxynitride perovskites, giving rise to notable electronic transport properties such as thermoelectricity in $\text{SrMoO}_{2-x}\text{N}_{1+x}$ ⁵ and colossal magnetoresistances (CMR) in $\text{EuNbO}_{2+x}\text{N}_{1-x}$ ⁶ and $\text{EuWO}_{1+x}\text{N}_{2-x}$.^{7,8} To discover whether the above anion order is stable to electron doping, we have explored stoichiometric d^1 materials, and we describe here the synthesis, magnetic properties and structure of a new oxynitride NdVO_2N containing $3d^1 \text{V}^{4+}$. Oxynitride perovskites were previously reported in the related $\text{LaVO}_{3-x}\text{N}_x$ system, but the reported samples had a maximum N content of $x = 0.9$.⁹

NdVO_2N was prepared by treating NdVO_4 precursors under NH_3 at a flow rate of $600 \text{ cm}^3 \text{ min}^{-1}$ at $700 \text{ }^\circ\text{C}$ for 80 hours with one intermediate regrinding. The colour of the new compound is black. Combustion analysis for the sample used for neutron diffraction gave a nitrogen content of 1.02 moles per formula unit. The X-ray diffraction pattern was indexed in an orthorhombic perovskite supercell of dimensions $a = 5.4596(7)$, $b = 5.5002(6)$ and $c = 7.7264(1) \text{ \AA}$ with space group *Pbnm* (see ESI†).

The magnetic susceptibility of NdVO_2N measured in a 1 T field shows paramagnetic behavior down to 2 K (Fig. 1), with no evidence of a spin ordering transition. The inverse susceptibility has a significant curvature,

indicating that both Curie–Weiss and temperature-independent paramagnetic contributions are present, and was fitted as $\chi^{-1} = [C/(T - \theta) + \chi_0]^{-1}$.

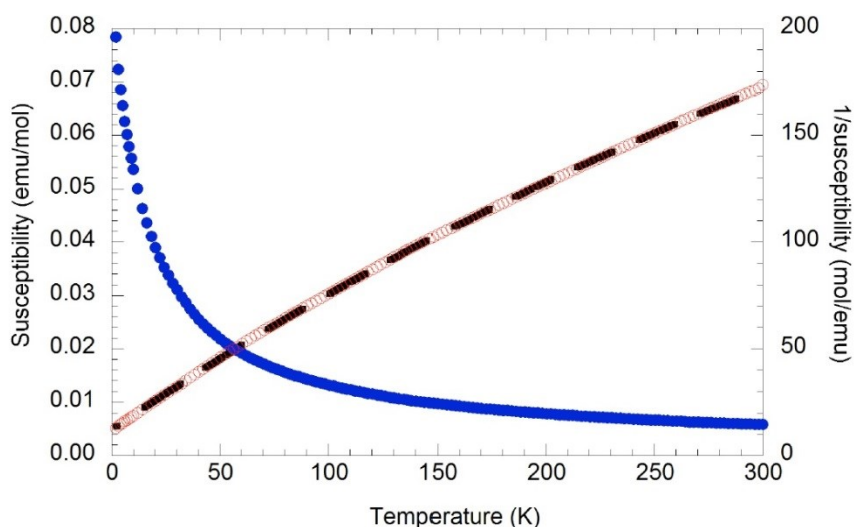


Figure 1. Magnetic susceptibility (closed points) and inverse susceptibility (open points) for NdVO₂N. The fit of the function described in the text to the inverse susceptibility is shown as a broken line.

The Curie–Weiss parameters ($C = 1.37 \text{ emu K mol}^{-1}$, corresponding to a paramagnetic moment of $3.32 \mu_B$, and $\theta = -17 \text{ K}$) describe localised $4f^3\text{Nd}^{3+}$ moments (ideal value $3.62 \mu_B$) with weak antiferromagnetic interactions. The large $\chi_0 = 0.0015 \text{ emu mol}^{-1}$ term reveals Pauli paramagnetism from correlated itinerant $\text{V}^{4+} 3d^1$ electron spins.

Powder neutron diffraction data for a 350 mg NdVO₂N sample (Fig. 2) were recorded at room temperature on a high-resolution diffractometer HRPD at the ISIS spallation source, Rutherford Appleton Laboratory, UK. Neutron profile refinements of the structural models and texture analysis were performed with the General Structure Analysis System (GSAS) software.¹⁰

The observed neutron diffraction peaks of NdVO₂N were consistent with an orthorhombic $\sqrt{2} \times \sqrt{2} \times 2$ superstructure of a cubic perovskite cell having space group $Pbnm$. This GdFeO₃-type superstructure is common in perovskites and results from two ordered tilts of the transition metal coordination octahedra. Distinct axial (Y1) anion sites, close to the c -axis, and equatorial (Y2) sites, near the ab -plane, are present in a 1 : 2 ratio. Refinement of their O/N occupancies subject to the overall composition gave values of 0.55(2)/0.45 and 0.73(1)/0.27, respectively. These occupancies are very close to those observed in SrMO₂N ($M = \text{Nb, Ta}$)¹ and evidence the same formation of *cis*-nitride chains as follows.

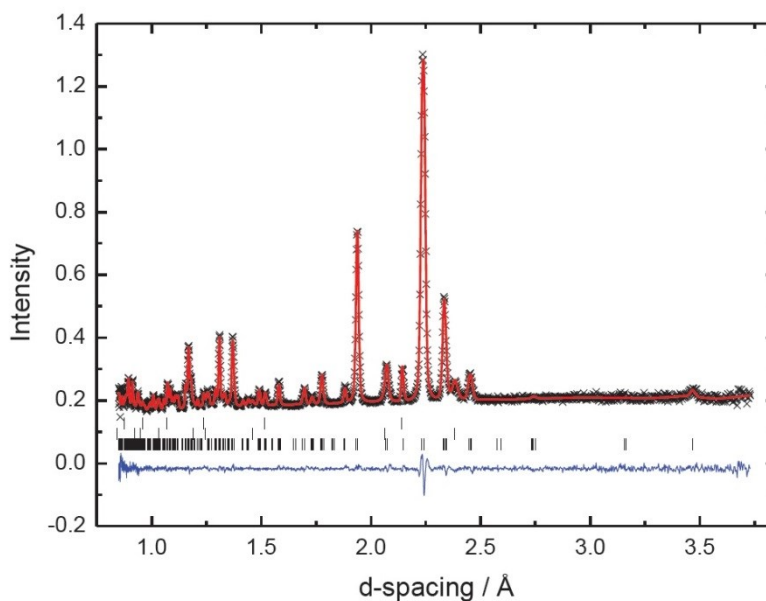


Figure 2. Fit of the monoclinic $P112_1/m$ model for NdVO_2N to powder neutron diffraction data from the 90° detector bank of instrument HRPD. Reflection markers from bottom to top are for NdVO_2N , a small amount of V(O,N) impurity phase, and scattering from the V sample holder.

Disordered $-M-N-$ chains with a 90° turn at M exist within perovskite layers in SrMO_2N and lead to statistical 0.5 O/0.5 N populations at the two anion sites in the layers and full 1.0 O occupancy at the third site between layers. The c -axis of the tilted $Pbnm$ superstructure lies in the anion-chain layers so that the axial Y1 O/N population is 0.5/0.5, and the equatorial Y2 population is averaged over in-chain-layer 0.5/0.5 and out-of-chain-layer 1.0/0 sites, giving 0.75/0.25 occupancy. The proximity of the refined anion site populations in NdVO_2N to these ideal values demonstrates that *cis*-VN chains are formed in the latter d^1 material.

A corollary of the anion-chain model is that the true space group symmetry of NdVO_2N is lower than $Pbnm$ because the equatorial Y2 sites are averaged over two anion positions with inequivalent (0.5/0.5 and 1.0/0) O/N occupancies. Breaking the equivalence of these sites lowers symmetry to monoclinic $P112_1/m$ (a non-standard setting of $P2_1/m$) with cell angle $\gamma \neq 90^\circ$.

We attempted to refine the $P112_1/m$ model but the monoclinic lattice distortion was found to be very small ($\gamma = 90.07^\circ$), so it was not possible to refine the full structure. However, by constraining the atomic coordinates to have $Pbnm$ pseudosymmetry, a refinement of split Y2-site occupancies converged, giving the results shown in Table 1. The refined Y2a and Y2b O/N occupancies of 0.90/0.10 and 0.50/0.50 are in excellent agreement with the prediction. Hence, the neutron analysis evidences a very small monoclinic distortion of the pseudo- $Pbnm$ perovskite superstructure of NdVO_2N driven by the anion-chain order.

Table 1. Atomic coordinates, anion site occupancies, and V–O/N bond distances for NdVO₂N refined in *P112₁/m* with *Pbnm* constraints

Site	<i>x</i>	<i>y</i>	<i>z</i>	O/N
Nda	0.0051(7)	0.0340(4)	0.25	
Ndb	0.4949	0.5340	0.25	
Va	0.5	0.0	0.0	
Vb	0.0	0.5	0.0	
Y1a	0.9348(6)	0.4864(4)	0.25	0.60(2)/0.40
Y1b	0.5652	0.9864	0.25	0.60(2)/0.40
Y2a	0.2838(4)	0.2890(4)	0.0382(3)	0.90(3)/0.10
Y2b	0.2162	0.7890	0.4618	0.50/0.50

Bond	Distance (Å)	Bond	Distance (Å)
Va–Y1b (×2)	1.968(1)	Vb–Y1a (×2)	1.968(1)
Va–Y2a (×2)	2.004(2)	Vb–Y2a (×2)	1.961(2)
Va–Y2b (×2)	1.959(2)	Vb–Y2b (×2)	2.002(2)

Estimated standard deviations in parentheses are shown once for each independent variable. Pairs of sites ending ‘a’ and ‘b’ are equivalent in the parent *Pbnm* structure and their coordinates were constrained accordingly. O/N occupation factors at the anion sites Y were refined subject to the ideal stoichiometry, and with equal occupancies at the Y1a and Y1b sites. Refined isotropic *U*-factors were 0.0009(3) Å² for metal atoms and 0.0067(3) Å² for anions. Refined cell parameters were *a* = 5.4645(3) Å, *b* = 5.5030(3) Å, *c* = 7.7352(4) Å, *γ* = 90.072(9)°.

Independent evidence for the lowering of symmetry was obtained from electron diffraction patterns of individual NdVO₂N crystallites of the powder. Many grains were twinned, but patterns from $\langle 110 \rangle_p$ zone axes of the cubic perovskite subcell were successfully obtained by tilting around the *c**-axis of single-domain crystallites (Fig. 3). These show additional weak reflections that result from loss of the glide planes, as symmetry is lowered from *Pbnm* to *P112₁/m*,¹¹ consistent with the neutron results. Double diffraction reflections along [001]* were also observed in these patterns.

The crystal structure of NdVO₂N is shown in Fig. 4. The octahedra are highly tilted with V–Y–V bond angles in the range 156–159°. The V–Y bond distances are slightly unequal, but similar differences are found in the *Pbnm* superstructures of NdMO₃ perovskites with non-degenerate ground state cations such as M = Cr³⁺ and Fe³⁺, so they are most probably a consequence of the tilting distortions and do not necessarily evidence a FOJT effect from V⁴⁺. A similar distribution of bond distances has been observed for metallic CaVO₃, which has *Pbnm* symmetry. The local order of O/N atoms into *cis*-VN chains within the crystallographically averaged V(O_{0.5}N_{0.5})₂ planes following the previously reported rules is shown on the right side in Fig. 4.

Randomized left/right turns of the chains at the V sites lead to the statistical averaging of the anion site populations within these layers.

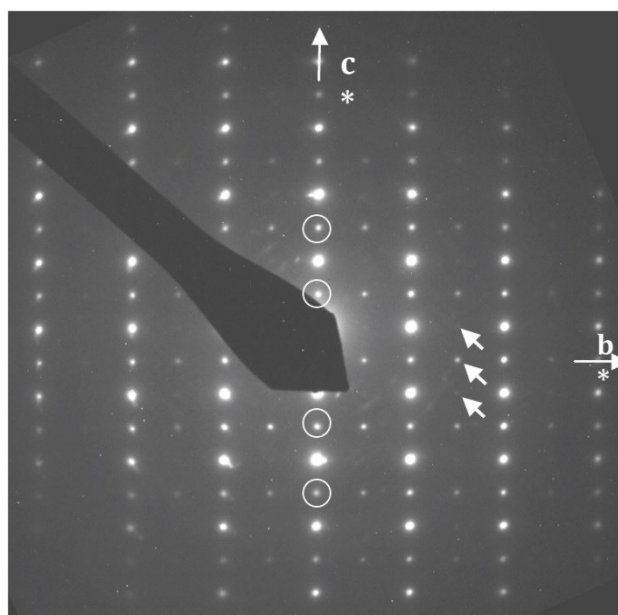


Figure 3. Electron diffraction pattern from a $\langle 110 \rangle_p$ cubic subcell zone axis, equivalent to the [100] axis for the $\sqrt{2} \times \sqrt{2} \times 2$ superstructure of a single-domain NdVO₂N crystallite. The presence of weak $0kl$; $k = 2n + 1$ reflections (diagonal arrows) shows that b-glide plane symmetry is broken, consistent with the descent from $Pbnm$ to $P112_1/m$ due to the anion order. Double diffraction reflections $00l$; $l = 2n + 1$ are indicated by circles.

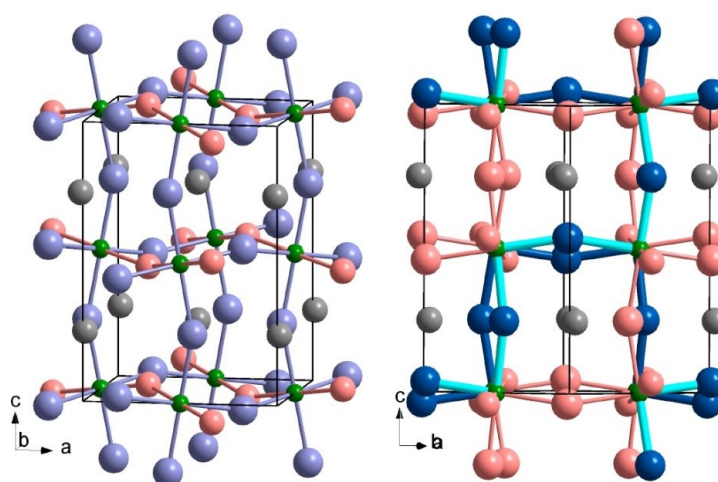


Figure 4. The tilted perovskite superstructure of NdVO₂N with Nd/V/O/O_{0.5}N_{0.5}/N sites shown as grey/green/pink/lilac/blue spheres. The left view shows the average $P112_1/m$ model with distinct O and O_{0.5}N_{0.5} sites, and local ordering of O/N atoms at the latter sites to give *cis*-VN chains is shown at the right with chains in one layer highlighted.

The discovery of anion order characteristic of planes of *cis*-nitride chains in NdVO₂N containing 3d¹ V⁴⁺ is significant as this order has previously only been established in insulating materials based on d⁰ ions. The chains in NdVO₂N result from corner-sharing of *cis*-VO₄N₂ octahedra, which are stabilised by strong SOJT type covalent interactions in *cis*-VN₂ units. *cis*-MX₂ groups formed by covalent bonding of d⁰ cations to two oxo or imido ligands X are very common in the coordination chemistry of high valent transition metals such as V⁵⁺ or Mo⁶⁺. d¹ analogues are rarer and are not known for V⁴⁺, but reported examples of *cis*-dioxomolybdenum(V) complexes¹² complement our observation that the *cis*-VN₂ geometry is preferred in NdVO₂N.

However, an important difference between *cis*-MX₂ units in molecular and extended solids is the possibility of itinerant electron behaviour in the latter case. AVO₃ perovskites and other V⁴⁺ oxides can show metallic and insulating properties. Perovskites of A = Ca, Sr, Cd and Mn are metallic without off-center V displacements, although a possible FOJT distortion was reported in MnVO₃.¹³ However, a pronounced SOJT off-center distortion to form a short V–O vanadyl bond was observed in insulating PbVO₃¹⁴ driven by cooperative displacements of lone pair Pb²⁺ cations. NdVO₂N appears to have features from both types of V⁴⁺ perovskite – the observed anion order implies that SOJT type covalent V–N interactions are significant, but the observed Pauli paramagnetism shows that the system is metallic, like most AVO₃ and electron-doped oxynitride perovskites. The *cis*-VO₄N₂ geometry is evidently robust to dopings into π*-bands formed from V:t_{2g} and O:2p_π orbitals of at least 1/6 electrons per V–O/N bond. It will be interesting to explore whether the anion order persists at higher electron concentrations, and in insulating d¹ analogues, if these can be synthesised. Spin and orbital states of localised d-electrons could be coupled to the O/N and octahedral tilt orders in the latter case, enabling novel electronic and magnetic properties to emerge.

In conclusion, this study has demonstrated that the structure of NdVO₂N contains layers of spontaneously segregated *cis*-nitride chains, like those in SrTaO₂N and other d⁰ oxynitride perovskites. The underlying formation of *cis*-VO₄N₂ octahedra is thus stable in the presence of the d¹ cation V⁴⁺. The 3d-electrons are itinerant in this material, so a future challenge is to design and explore the properties of perovskite oxynitrides in which spin and orbital states of localised d-electrons may be coupled to the O/N and octahedral tilt orders.

References

- [1] M. Yang, J. Oró-Solé, J. A. Rodgers, A. B. Jorge, A. Fuertes and J. P. Attfield, *Nat. Chem.*, 2011, **3**, 47.
- [2] A. Fuertes, *J. Mater. Chem.*, 2012, **22**, 3293.
- [3] S. G. Ebbinghaus, H.-P. Abicht, R. Dronskowski, T. Müller, A. Reller and A. Weidenkaff, *Prog. Solid State Chem.*, 2009, **37**, 173.
- [4] P. J. Camp, A. Fuertes and J. P. Attfield, *J. Am. Chem. Soc.*, 2012, **13**, 6762.
- [5] D. Logvinovich, R. Aguiar, R. Robert, M. Trottmann, S. G. Ebbinghaus, A. Reller and A. Weidenkaff, *J. Solid State Chem.*, 2007, **180**, 2649.
- [6] A. B. Jorge, J. Oró-Solé, A. M. Bea, N. Mufti, T. T. M. Palstra, J. A. Rodgers, J. P. Attfield and A. Fuertes, *J. Am. Chem. Soc.*, 2008, **130**, 12572.
- [7] A. Kusmartseva, M. Yang, J. Oró-Solé, A. M. Bea, A. Fuertes and J. P. Attfield, *Appl. Phys. Lett.*, 2009, **95**, 02110.
- [8] M. Yang, J. Oró-Solé, A. Kusmartseva, A. Fuertes and J. P. Attfield, *J. Am. Chem. Soc.*, 2010, **132**, 4822.
- [9] P. Antoine, R. Assaba, P. L'Haridon, R. Marchand, Y. Laurent, C. Michel and C. B. Raveau, *Mater. Sci. Eng.*, 1989, **B5**, 43–46.
- [10] A. C. Larson and R. B. Von Dreele, *Los Alamos National Laboratory Report No LAUR*, 1994, pp. 86–748.
- [11] D. I. Woodward, P. L. Wise, W. E. Lee and I. M. Reaney, *J. Phys.: Condens. Matter*, 2006, **18**, 2401.
- [12] X.-M. Lu, J.-F. Lu and X. A. Mao, *Chin. J. Chem.*, 2002, **20**, 617.
- [13] M. Markkula, A. M. Arevalo-Lopez, A. Kusmartseva, J. A. Rodgers, C. Ritter, H. Wu and J. P. Attfield, *Phys. Rev. B: Condens. Matter Mater. Phys.*, 2011, **84**, 094450.
- [14] (a) R. V. Shpanchenko, V. V. Chernaya, A. A. Tsirlin, P. S. Chizhov, D. E. Sklovsky, E. V. Antipov, E. P. Khlybov, V. Pomjakushin, A. M. Balagurov, J. E. Medvedeva, E. E. Kaul and C. Geibel, *Chem. Mater.*, 2004, **16**, 326; (b) A. A. Belik, M. Azuma, T. Saito, Y. Shimakawa and M. Takano, *Chem. Mater.*, 2005, **17**, 269